Characterization & Monitoring at FRC Area 3 using Geophysical Data Conditioned to Hydrogeological Data

Susan Hubbard, Jinsong Chen, John Peterson and Ken Williams (LBNL)
David Watson and Phil Jardine (ORNL) and Michael Fienen (Stanford)
August, 2003

1. Introduction

High resolution crosshole radar and seismic data have been (and are being) collected at Area 3 of the ORNL Nabir FRC. The primary objectives of the geophysical component of the FRC biostimulation project is to use the geophysical data, constrained to direct hydrogeological measurements, to provide characterization input for the flow and transport model. Previous work has shown that estimates of hydraulic conductivity obtained from geophysical data are extremely useful for improving flow and transport predictions, even in fairly homogeneous aquifers and replete with borehole data (Schiebe and Chien, 2003). A secondary objective of the geophysical component of the project is to use time-lapse geophysical data to monitor system transformations that could occur during the biostimulation, such as changes in the pore fluid, gas generation, or precipitate development.

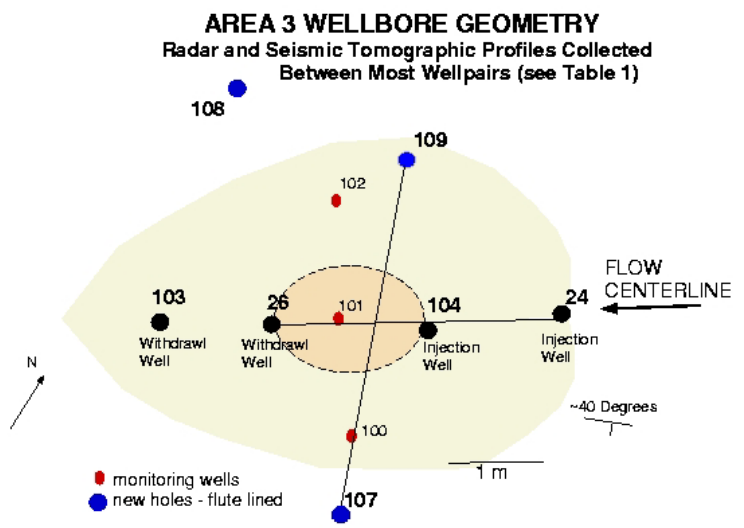

Figure 1. Examples of tomographic profiles relative to the biostimulation injection and withdrawal wells are shown in this figure. However, as described in The Appendix, seismic and radar tomographic data have been collected between most wellpairs.

As shown in the Appendix, data were collected during three different acquisition campaigns at the FRC. Limited data were collected in 2001 to test signal penetration. In the Fall of 2002, the three 'geophysical' holes were drilled (107, 108 and 109; see Figure 1), hole 104 was re-drilled, and a chemical tracer test was performed. Seismic and radar tomographic data were collected in 2002 directly after the redrilling and tracer test activities at the FRC. As will be discussed in Section 3, system perturbations resulting from these activities were detectable on the tomographic data. As such, data were again collected in 2003 to assess the validity of using the 2002 data as 'baseline' information for the hydrogeological characterization.

In this document, we describe the hydrogeological estimates that we have obtained from the geophysical data, and illustrate the sensitivities of the radar and seismic attributes to system transformations associated with the pre-stimulation activities at the site (tracer test & drilling). Our analysis suggests that the geophysical data are useful for delineating the targeted fracture zone in 3-D. Our analysis also suggests that the geophysical data will be useful for monitoring the transformations that occur during the biostimulation. The initial phase of the biostimulation experiment (the acidified water flush) is currently being performed, and we are monitoring it using time-lapse seismic and radar

data to image the change in pore fluids as the native groundwater is replaced by the injectate. Funding permitted, we hope to also monitor the stimulation portion of the experiment.

2. Geophysical Signatures of the Stimulation Zone

Figure 2 illustrates examples of seismic and radar tomographic data, both collected along the injection centerline between wellbores 24-26 (see Figure 1). This figure illustrates that the stimulation zone can be delineated using the geophysical data, and that, relative to the surrounding formation, the stimulation zone exhibits both low seismic and radar velocities. An electromagnetic flowmeter log, collected at well 24, is also shown in Figure 2, which illustrates that the stimulation zone is associated with high hydraulic conductivity (K) values. Low seismic velocity values are the expected response in a fractured (less 'stiff') material surrounded by a more cohesive material, as is the case with the stimulation zone. It should be noted that inversion of the FRC tomographic data was difficult, requiring significant geophysical anisotropy and wellbore deviations corrections.

Figure 2

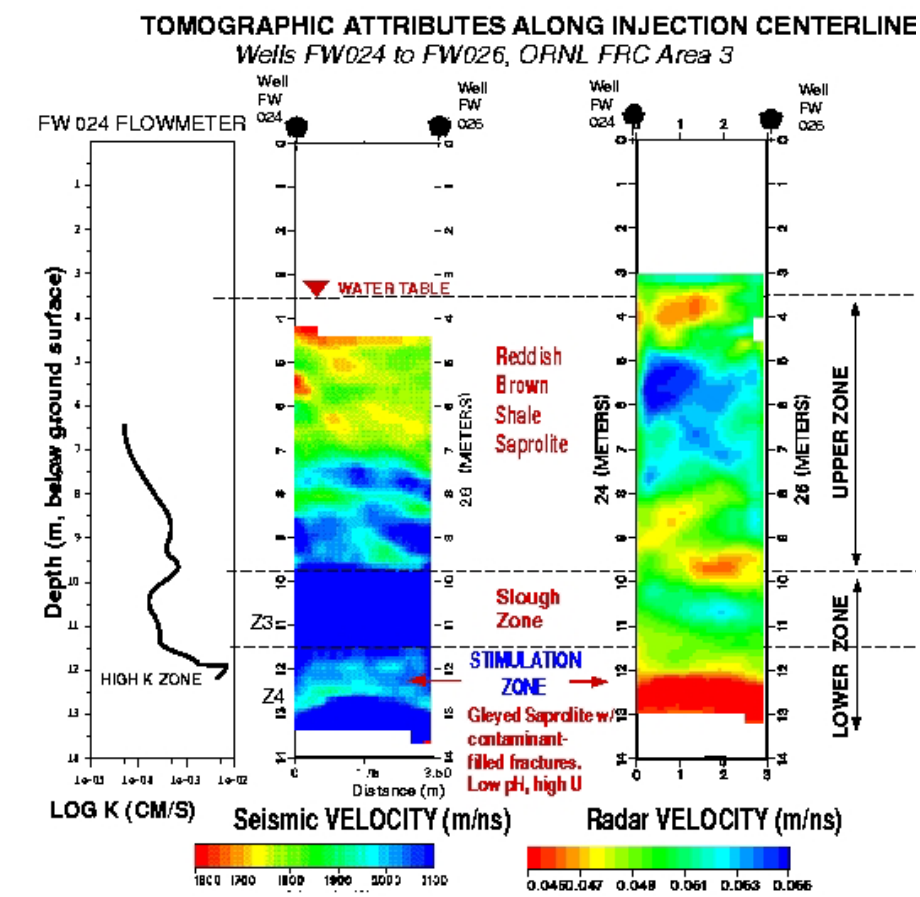

We used the seismic data to investigate the spatial heterogeneity of the stimulation zone for several reasons: the seismic data were of better quality than the radar data in general, seismic data appear to be more sensitive to the presence/absence of fractures than the radar data, and because we had more complete coverage of the seismic data from the 2002 experiment (see the Appendix). Figure 3 illustrates seismic velocity fence diagrams, or cross sections, along geologic strike and dip direction. The upper figure shows the seismic velocity primarily along the dip direction, between, wellbores 107 and 109 (refer to Figure 1), while the lower figure shows the seismic velocity signature along the strike direction (between wells 24-26). The 'red' low velocity layer indicates the stimulation zone. This zone appears to be laterally variable in both thickness and in seismic velocity (and thus hydraulic conductivity) values. Thicker zones of lower velocity (i.e., higher hydraulic conductivity) are apparent toward the north of the centerline in the inner flowzone (see Figure 1), while the zone appears to thin and to even be discontinuous towards the south.

3. Hydrogeological Heterogeneity

Our goal is to use the geophysical data, such as those shown in Figures 2 and 3, to estimate hydrogeological parameters that can be used to constrain the flow and transport model. Several data sets were available for analysis, including the tomographic data and gamma ray and flowmeter borehole data. Below, we briefly review the available borehole data (Section 3.1), and then discuss interpretation of the seismic data in terms of hydrogeological heterogeneity (Section 3.2). Section 3.3 compares the geophysical-obtained estimates of hydrogeological heterogeneity with the tracer test breakthrough data as a qualitative validation of our estimation approach.

Figure 3

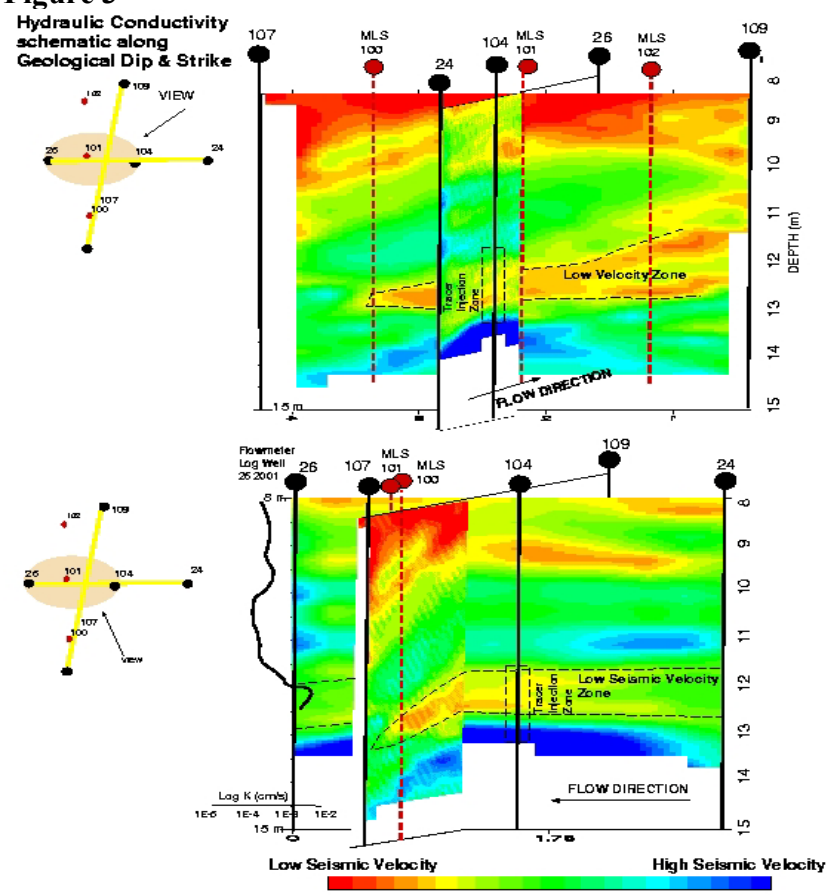

3.1 Analysis of Borehole Data

Figure 4 shows natural gamma-ray logs collected at many of the wells in the study area, where high gamma ray values are indicative of clay-rich areas. These logs reveal the existence of two major geological zones at this site: an upper layer and a lower layer, with an interface between the two at ~8-10 m, depending on the location within the study area and the geological dip. The upper layer has a

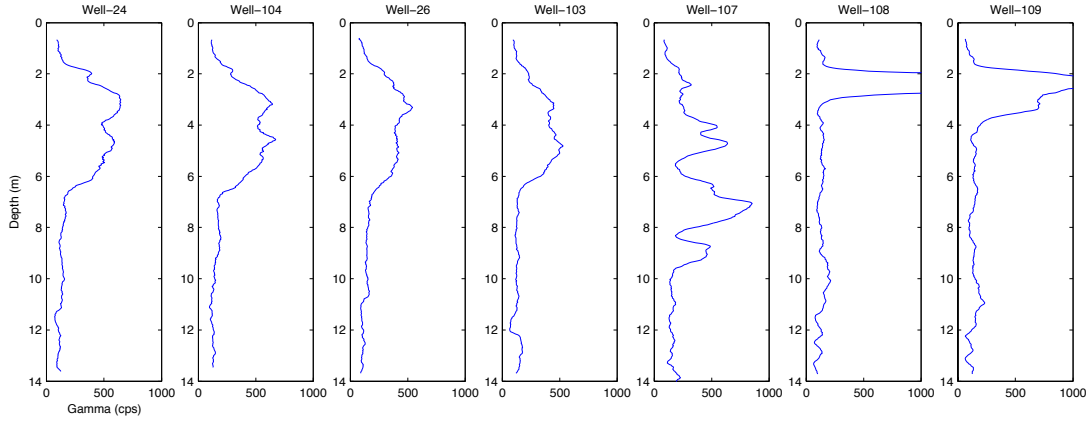

Figure 4. Gamma ray counts along seven wellbores. Provided by David Watson, ORNL.

high clay content, whereas the lower layer has lower clay content. The zonation between the upper and lower layer can be observed on the geophysical tomograms shown in Figure 2. Because the stimulation zone is located within a highly fractured zone in the 'lower' layer, for our subsequent discussions we focus primarily on interpreting variability within this layer only.

Electromagnetic flowmeter data were used to assess the hydraulic conductivity in the vicinity directly around the wellbores. Figure 5 shows indicator hydraulic conductivity values along each wellbore. These logs were constructed using the median of the flowmeter measurements (along wellbores 24, 26, 103, 104, 107, 108, and 109) as the cutoff value (2.8E-5 cm/s). We chose to use an indicator representation of the flowmeter logs because the quality of the quantitative flowmeter data (i.e., exact value of hydraulic conductivity) varied between the different wellbores due to different well completion procedures, while qualitative information about the presence or absence of a high conductivity unit was reliable. The flowmeter data suggest that the high conductivity zone along the flow centerline is about 1m thick, and the center of the zone along the centerline is located at about 11.8m. The flowmeter data also suggest that there are variations in the thickness of the high permeability zone, depending on location within the study site.

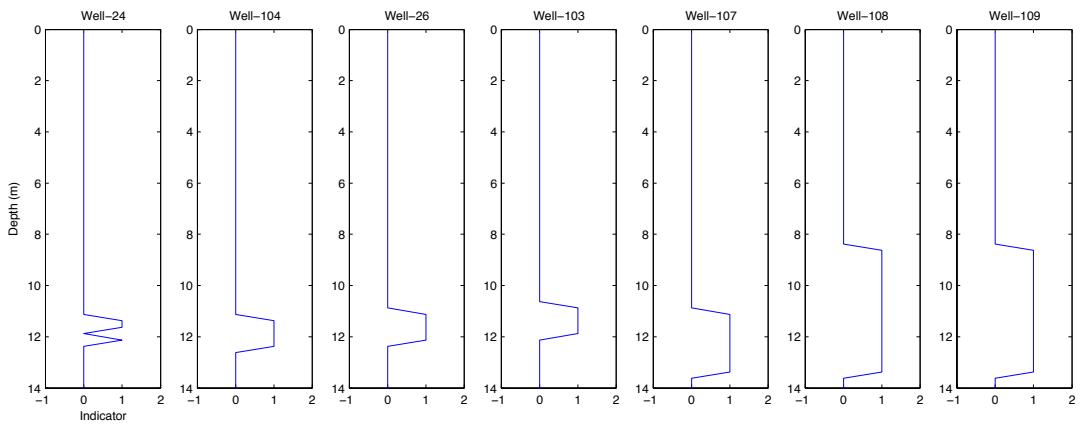

Figure 5. Flowmeter data along seven wellbores expressed in terms of indicator hydraulic conductivity, with 'high' values being greater than 2.8E-5 cm/s, and 'low' values being lower than that. As the top of the packing depth for wells 103 and 104 is at 37ft (11.3m), the upper boundary of the high permeability zone is uncertain at these locations. Modified from flow measurements collected by ORNL (David Watson) and Michael Fienen (Stanford).

3.2 Estimation of hydrogeological Heterogeneity using seismic tomographic Data

In this section, we use seismic travel time data in conjunction with flowmeter measurements to delineate the zonation of the high conductivity zone away from the borehole. This information can be used within the flow and transport model, as well as to help us qualitatively understand the field-scale flow and tracer experimental results.

To estimate hydraulic conductivity using seismic data, we typically first develop relationships between hydraulic conductivity and geophysical attributes based on co-located data collected at boreholes. This approach has been successful for estimation of hydrogeological parameters using geophysical data in porous granular materials (e.g., Chen et al., 2001; Hubbard et al., 2001). However, developing such relationships with confidence at this fractured site proved difficult. We suspect that the difficulty was due to the different sampling volumes of the borehole flowmeter data and the

geophysical data, which is exacerbated by the presence of fractures. The wellbore flowmeter data sense the local fractures, which are spaced asymmetrically around the wellbores, whereas seismic data sense the fracture zones in an effective manner over the distance between the two boreholes. As an example, Figure 6 shows the seismic velocity versus depth for the area (pixels) near wellbore 107 extracted from all tomograms that intersect wellbore 107 (refer to the Appendix and Figure 1). It is clear that the seismic data are not sensing the fracture distribution in the near vicinity of wellbore 107 only (as are the flowmeter data), as the values are quite different depending on the direction of the tomogram. This concept of how the measurement support scales of the different data sets influence what aspect of the fracture system is detected is schematically illustrated in Figure 7.

Figure 6

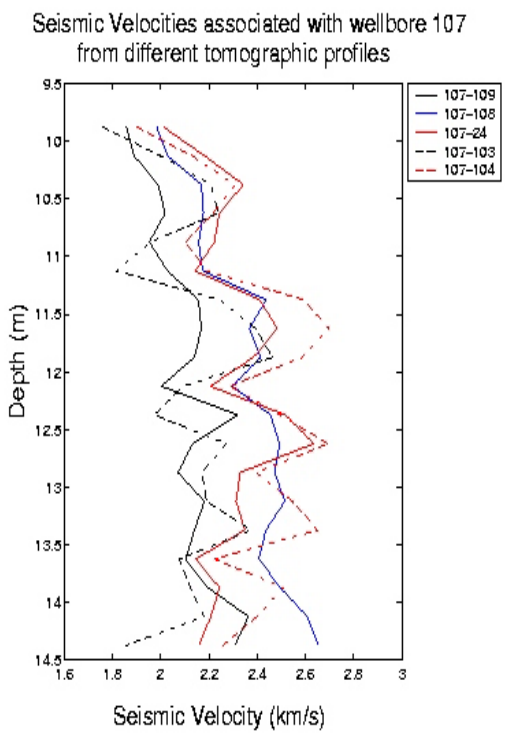

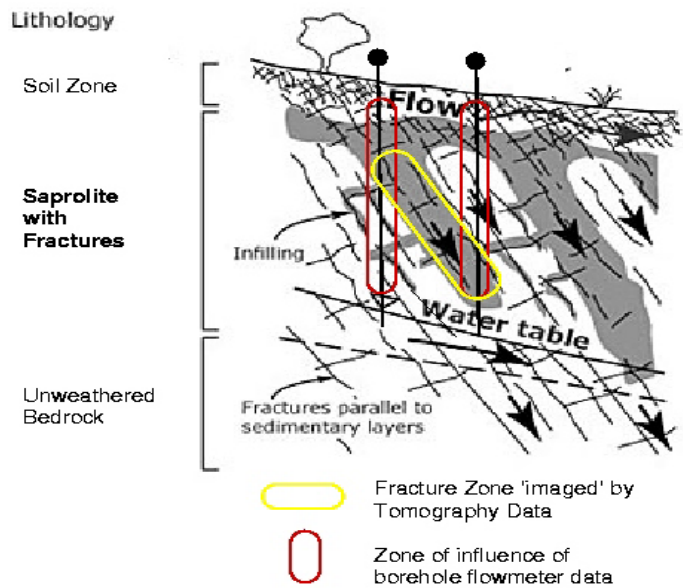

Figure 7 Schematic illustration showing the influence of the fracture system on the borehole and tomographic data sets as a function of measurement support scale. Conceptual model of saprolitic system from the University of Tennessee Hydrology Program (Larry McKay; http://web.utk.edu/~hydro/Saprolites/)

Because of this sampling inconsistency in the presence of fractures and because of the uncertainties associated with what we consider to be the 'true' data (the electromagnetic flowmeter data), we choose to estimate the hydrogeological zonation rather than continuous values of hydraulic conductivity. We choose to estimate the probability of observing the high permeability fracture zone, defined as being over a threshold hydraulic conductivity value determined from the log data. Estimation of the fracture zonation should be quite useful in predicting flow and transport at this site. Indeed, in a study that investigated the worth of data hydrogeological investigations, James and Freeze (1993) stated that *'when it comes to hydrogeological parameters….the sensitivity analysis indicates that it is more important to know whether the field value is above or below some threshold value than it is to know its actual numerical value*'.

We developed a Bayesian model based on the Monte Carlo Markov Chain (MCMC) method to estimate hydraulic conductivity indicator values by using seismic travel time data and flowmeter

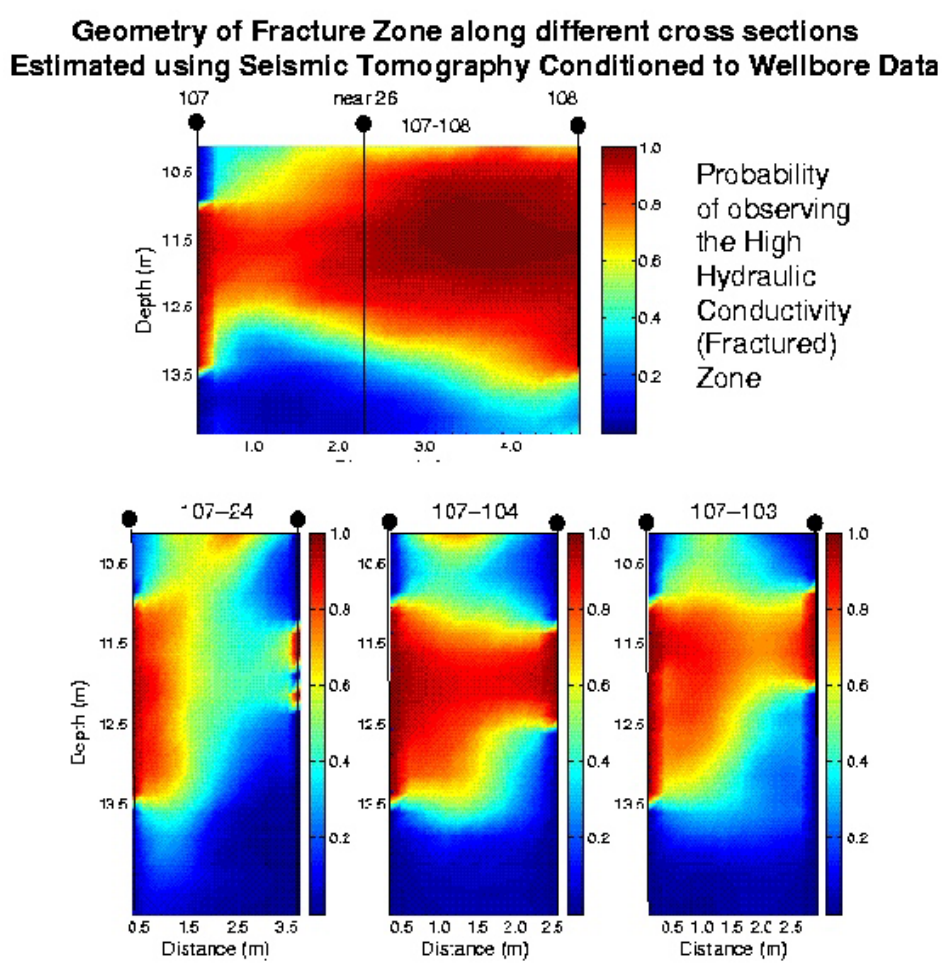

Figure 8

measurements at each wellbore. Seismic velocity information and hydraulic conductivity indicator values at each location between wellbores were considered as random variables. We estimated the probability of observing the high hydraulic conductivity zone at each pixel by conditioning to hundreds to thousands of cross well seismic travel time data and borehole flowmeter data. The detailed methodology will be presented at the Fall AGU meeting in San Francisco (Chen et al., 2003b) and in a journal paper, which is in development. The methodology is an extension of other approaches that we have recently developed to estimate aquifer parameters using the Bayesian model (Chen et al., 2003a; Chen et al., 2003b). For brevity, we refer to these references rather than report the mathematical development of the approach here. Figure 8 shows the estimated probability of observing the high hydraulic conductivity zone along many cross sections in the study area (refer to Figure 1). These figures suggest that the high permeability stimulation zone has a varying thickness, variable dips, and is sometimes laterally discontinuous. We expect that these variations will influence transport direction and breakthrough times.

3.3 Comparison of Geophysically-obtained Estimates with Breakthrough Data

To qualitatively assess our estimated results, in this section we compare the estimated probability of high hydraulic conductivity zone with the observations of field-scale tracer experiments. The tracer experiment was performed in November of 2002 and involved an initial calcium chloride flush from wellbore 24 through the lower zone of interest and within the inner and outer flowcells. This flush was followed by an Fe(III) and bromide tracer test, where the tracers were injected into wellbore 104 between 11.3 and 13.7 m below ground surface, and were monitored at the multilevel samplers located

at 100, 101, and 102 (refer to Figure 1), as well as downgradient wells. In this discussion, we work only with the conservative bromide tracer results.

Figure 9 shows a comparison of the estimated high conductivity zonation along geologic dip, with the locations of the multi-level sampler projected onto the figure, sometimes from out of the plane (refer to Figure 1). Comparison of Figure 9 with Figure 3 (top) shows the differences between the geophysical image of the stimulation zone and the estimated hydrogeological zonation using the geophysical data constrained by wellbore information within the Bayesian approach. As shown in Figure 9, the three ports of each multi-level sampler well had a 0.91m sampling interval, with the centers of the ports at depths 10.2m, 11.7m, and 13.2m, respectively. Because of the sparse sampling of the tracer test data, we were not able to calculate the movement of the tracer plume center of mass. However, analysis of the breakthrough data suggested that the majority of the tracer mass moved from the injection well towards the north, or between sampling wells 101 and 102, and that much less mass moved towards the south, or between wells 100 and 101 on Figure 8. Thus, the centerline of mass movement did not coincide with the flow centerline (see Figure 1), but instead veered northward.

Figure 9 offers some explanation of this transport direction. Consider that the tracer was injected into well 104, which is along geologic strike from well 101, which is annotated on Figure 9, and over the same depth intervals as the center sampler of well 101. The probability of the presence of

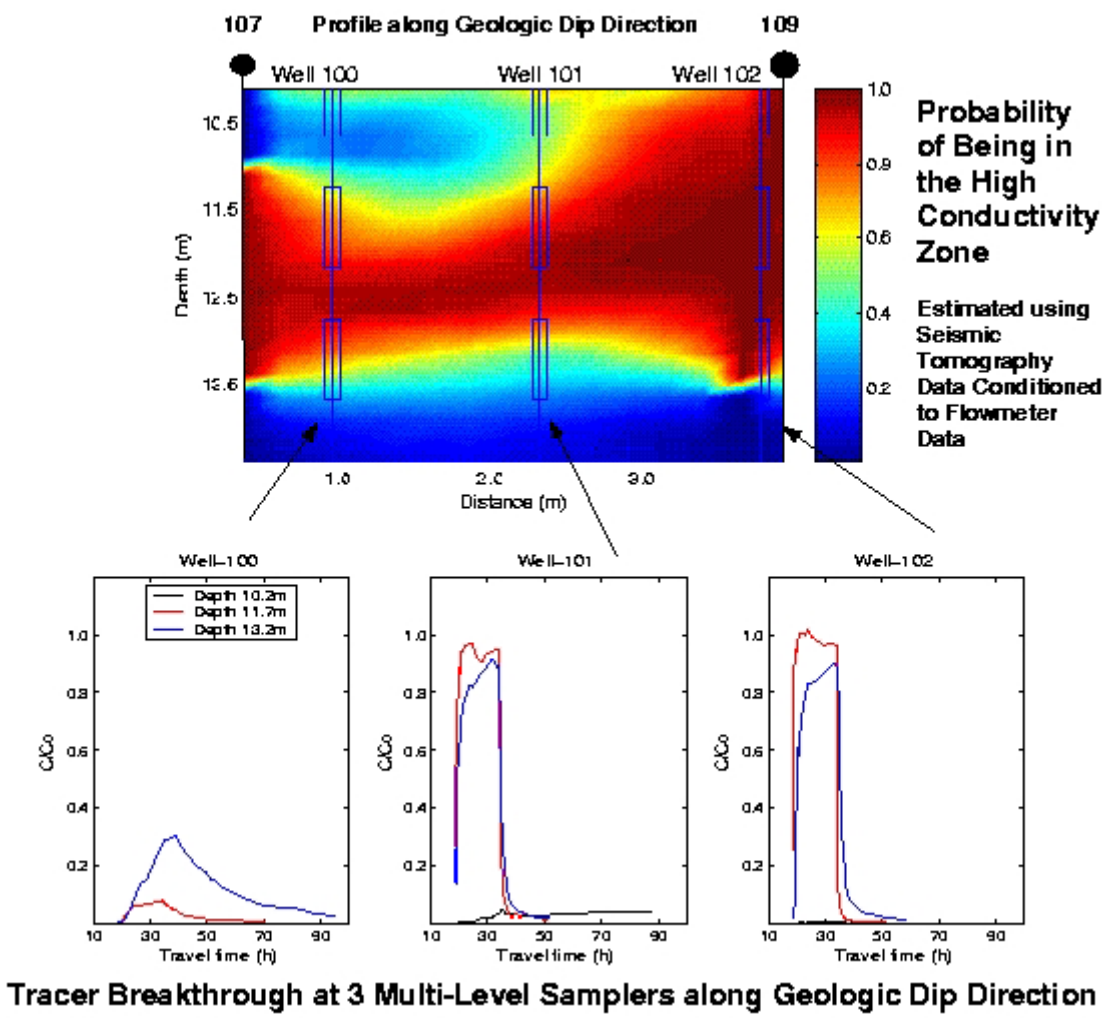

Figure 9 Comparison of fracture zone geometry and breakthrough data along transect between wells 107 and 109. Tracer test data provided by ORNL.

the high permeability zone is much greater to the north (between wells 101-102) and there is thicker zone there than what is observed to the south (wells 100-101). Keep in mind that this plot indicates the probability of observing the high permeability layer, or where the layer is 'more likely' to be observed, rather than representing the absolute geometry of the layer. The breakthrough curves for the three ports in each well are shown on the bottom of Figure 9. These figures show that at wells 101 and 102, the upper and middle ports, which are located within the thicker portions of the estimated high permeability zone, received most of the tracer, and the lower port did not sample much tracer. The downdip well, well 100, which is located south of a thin (pinched-off?) section of the layer, did not receive significant tracer mass at any of the ports. Although some of these multi-leveler samplers are projected into the zonation plot on Figure 9 from out of the plane, the zonation geometry seems to have influenced tracer transport.

4. Monitoring Changes in System during Perturbations

In addition to providing characterization data, which can be used to constrain the flow and transport model and to qualitatively understand the tracer test experiment, we are also interested in using time-lapse geophysical data to monitor system transformations that may occur during the stimulation. These changes may be caused by, for example, changes in the pore water chemistry, development of precipitates, and gas generation associated with denitrification. The stimulation test is starting now and we are monitoring it. As such, we can not report monitoring results. We can, however, report the relative sensitivities of the geophysical data due to some of the system perturbations that have already occurred at the site due to drilling activities and the tracer test.

Figure 10

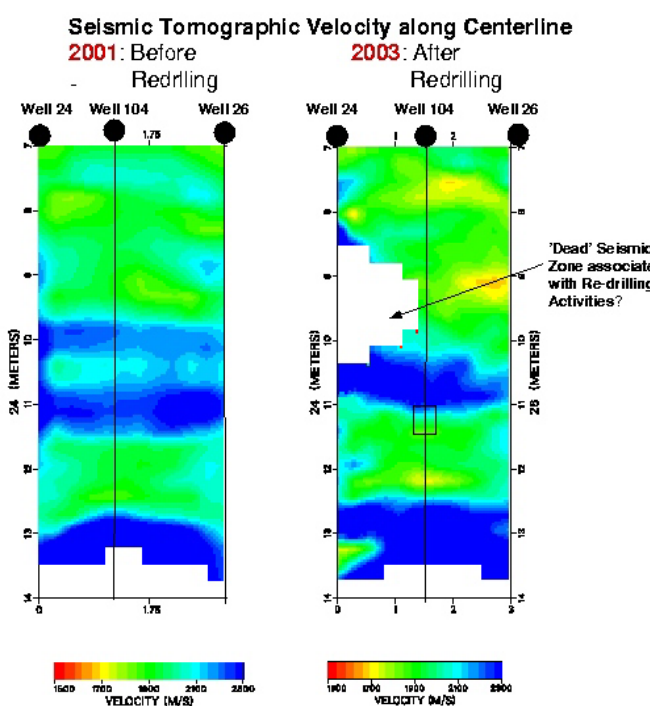

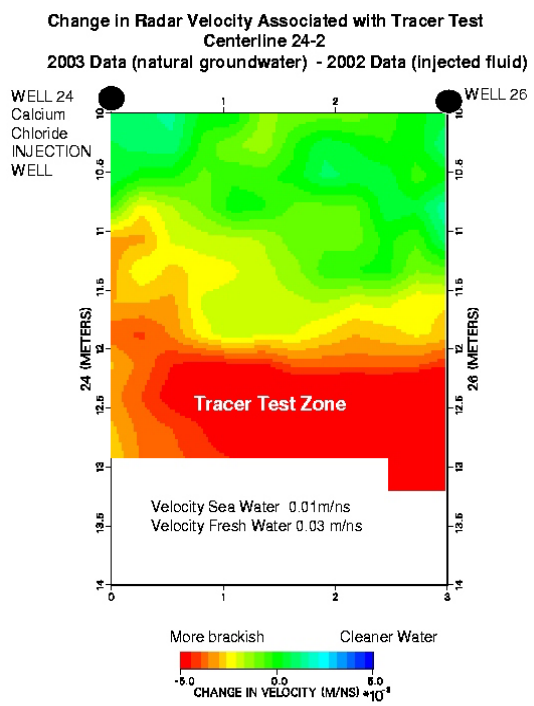

Figure 11

Figure 10 shows seismic velocity tomograms collected along the injection centerline (from wells 24-26) in 2001 and again in 2003. Between this time (in October of 2002), wellbore 104 was redrilled. During the redrilling, at a depth of 11.3m below ground surface (see rectangle on the 2003 tomogram in Figure 10), fluids started to come up out of the hole on well 24 and well 102, indicating that the subsurface section had been over pressurized. The presence of drilling gas or ruptured rock due to the redrilling incident would tend to decrease the seismic amplitudes to a point where they are not recognizable on the seismic records, which is the response indicated by the white zone on Figure 10. Although this zone, interpreted to be a zone of disturbance from the drilling activity, is above the stimulation zone, Figure 10 illustrates the utility of the seismic data to detect changes in the subsurface due to either gasses or stiffness, which are two of the responses that we expect if gasses or precipitates are generated during the stimulation.

Radar velocities appear to be quite sensitive to the pore fluid electrical conductivity at this FRC site. Figure 11 shows the change in the radar velocity along the centerline cross section (wells 24-26), calculated by differencing the velocities detected in 2002 (directly after the tracer test, which injected 'cleaner' water than the native groundwater) from those recorded in 2003 (after the system had been restored to natural conditions of high ionic strength groundwater). The red zone shows that the pore fluids in 2002 (associated with the tracer test) were fresher (higher velocity) than those measured in 2003, after the groundwater had returned to natural conditions. This plot suggests that the radar data should be quite useful for monitoring at the FRC, such as during the acidified water flush.

5. Summary

We have used seismic and radar tomographic data, constrained by borehole data, to interpret the hydrogeological zonation in Area 3 of the FRC, and to assess system perturbations that have been detected due to pre-stimulation experiments. Our experience with seismic/radar acquisition and inversion in various subsurface environments suggests that the FRC Area 3 hydrogeology is extremely heterogeneous, but that the data can be used to delineate the high permeability fracture zonation. Analysis of time-lapse geophysical data suggest that the radar data appear to be very sensitive to changes in pore fluid chemistry, and thus should be useful in a constrained monitoring mode during the biostimulation, and that the seismic data, in addition to being useful for hydrogeological heterogeneity zonation, should be useful for detecting gasses or precipitates that may develop during the stimulation. In summary, our analysis suggests that:

- ***The high conductivity stimulation zone varies in thickness, dip, and continuity throughout this small study area. Comparison of the estimation results with the tracer data suggests that the heterogeneity controlled transport at this site.***

- ***Time-lapse geophysical data can also be very useful for monitoring changes that occur in a system due to perturbations.***

6. Future Work

Funding permitting, we would like to continue to monitor the biostimulation experiment through the Winter of 2003. In addition to hydrogeological heterogeneity, as was discussed above, it is well recognized that heterogeneity of biogeochemical parameters is typically great and is characterized by multiple spatial scales. In addition to these natural variabilities under static conditions, the biostimulation experiment will induce dynamic biogeochemical and hydrological transformations in

the subsurface. As difficult as it is to use conventional approaches to characterizing or monitoring hydrological parameters/processes, it seems ever so much more difficult to capture the spatial and temporal variability of biogeochemical reactions using conventional point measurements, which often only reflect very localized conditions. The inability to collect the necessary hydrogeological-biogeochemical measurements using conventional characterization tools, at a high enough spatial resolution yet over a large enough volume, severely inhibits the ability to assess the efficacy of the remediation and the zone of influence.

Geophysical methods hold promise for rapid, non-destructive, relatively inexpensive and vastly improved monitoring of system transformations that can occur during remediation. At the FRC, the data should be useful for helping to understand many components of the experiment. For example, we will use the time lapse geophysical data to assess the efficacy of the groundwater flush, which is being performed to remove undesirable chemicals prior to the stimulation. Changes in seismic and radar attributes should also be useful for helping to understand:

- The performance of the ex-situ treatment facility to successfully remove components such as nitrate from the natural groundwater;
- If re-oxidation occurs after treatment;
- Assessing if large quantities of uraninite are precipitated within the biostimulation re-circulation cell;
- Delineating the boundaries of the inner and outer flow cells; and
- Determining when and where aluminum hydroxide and/or urananite precipitation is occurring.

Geophysical imaging of coupled biogeochemical-hydrological processes is a new area of research and as such, is still in its infancy. However, based on the evidence presented in Section 4, we suspect that time-lapse geophysical data, constrained by sparse but direct measurements, could be extremely useful for helping to understand the system transformations over space and time at the FRC Area 3. Additionally, an improved ability to characterize and monitor subsurface parameters and processes that occur over a variety of spatial scales using geophysical data, developed through experiments such as this one, will reduce the uncertainty currently associated with the efficacy of many remediation treatments at other DOE sites.

7. References

Chen, J., Hubbard, S., Rubin, Y., Murray, C., Roden, E. and Majer, E., Geochemical characterization using geophysical data: a case study at the South Oyster Bacterial Transport Site in Virginia, in revision with *ES&T*, 2003a.

Chen, J. et al., Estimation of Hydrogeological Zonation at the NABIR Field Research Center (FRC) using high-resolution geophysical data within a Monte Carlo Markov Chain Approach, *EO*S, Dec. 2003b.

Chen, J., S. Hubbard and Y. Rubin, Estimating Hydraulic Conductivity at the South Oyster Site from Geophysical Tomographic Data using Bayesian Techniques based on the Normal Linear Regression Model, *Water Resources Research*, 37(6), 1603-1613, 2001.

Chen, J. and M. Hoversten, Joint stochastic inversion of geophysical data for reservoir parameter estimation, SEG extended abstract, 2003.

Hubbard, S., Chen, J., Peterson, J., Majer, E., Williams, K., Swift, D., B. Mailliox and Y. Rubin, Hydrogeological Characterization of the D.O.E. Bacterial Transport Site in Oyster Virginia using Geophysical Data, *Water Resources Research,* 37(10), 2431-2456, 2001.

James, B.R. and R.A. Freeze, The worth of data in predicting aquitard continuity in hydrogeological design, *Water Resources Research*, 29(7), 2049-2065, 1993.

Scheibe, T.D., and Y. Chien, An evaluation of conditioning data for solute transport prediction, *Ground Water*, 41(2), 128-141, 2003.

APPENDIX.
Crosshole Geophysical Acquisition using both seismic and radar methods at the FRC Area 3.

Acquisition YEAR:	2001		2002*		2003	
Geop. METHOD: Borehole PAIRS (see Fig. 1)	Seismic	Radar	Seismic	Radar	Seismic	Radar
107-104			x			x
107-103			x			
104-103			x-PQ		x-PQ	x
108-103			x			x
108-107			x	x		
109-107			x	x	x	
108-104			x-PQ	x		x
108-24			x-PQ			
107-24			x			
24-26	x	x**		x	x	x
108-109					x	x
24-109					x	x
108-26					x	

Unless otherwise indicated, full tomographic data were collected to yield a 2-D distribution of parameters between the wellbore pairs with a resolution of ~1/4m by 1/4m.

KEY:
PQ - Poor quality; data acquisition was attempted but not completed. The quality is interpreted to be associated with 2001 field activities (drilling disturbance/gas generation).
**Zero Offset Profile collected only, which is one trace for each transmitter-receiver pair, located at sequential depths down the borehole to yield average horizontal velocity information as a function of depth (1D).